

Stereodynamics in Dissociative Adsorption of NO on Si(111)

M. Hashinokuchi,¹ M. Okada,^{1,2,*} H. Ito,¹ T. Kasai,¹ K. Moritani,³ and Y. Teraoka³

¹Department of Chemistry, Graduate School of Science, Osaka University, Toyonaka, Osaka 560-0043, Japan

²PRESTO, Japan Science and Technology Agency, Kawaguchi, Saitama 332-0012, Japan

³Synchrotron Radiation Research Center, Japan Atomic Energy Agency, Sayo, Hyogo 679-5148, Japan

(Received 27 January 2008; published 25 June 2008)

We report results of our study on the surface-temperature dependence of the steric effect in the dissociative adsorption of NO on Si(111)-(7 × 7). Data presented here show that, at an incident energy of 58 meV, the reactive sticking probability for the N-end collision is larger than that for the O-end collision. Furthermore, this steric preference is quite sensitive to the surface temperature and the surface coverage. This study shows that the transient surface trapping into a shallow precursor well plays a key role in the stereodynamics of the dissociative adsorption at the low energy region.

DOI: [10.1103/PhysRevLett.100.256104](https://doi.org/10.1103/PhysRevLett.100.256104)

PACS numbers: 68.49.Df, 34.35.+a, 68.43.-h, 68.47.Fg

The steric effect, reactant orientation, and alignment, are of great importance in surface chemistry [1–15]. The stereodynamics of NO on a surface has been a particular target of several studies using various experimental approaches [1–7]. In the scattering of NO from the inert Ag(111) [1,4], the corresponding orientation-dependent interaction potential accounted for the observed steric effects and the resultant rotational excitation of scattered NO. In the reactive NO/Pt(111), the trapping probability is higher for the N end than for the O end [2]. The sticking probability of NO on reactive Ni(100) and Pt(100) also demonstrated that the N end is more reactive than the O end [3,5,7]. Moreover, clear steric effects have been observed in the gas-phase products for the (NO + CO) reactions on Pt(100) [6]. In these experiments, little attention was given to the surface products. However, it should be noted that an elucidation of the molecular-orientation effects in the reaction products on the surface is necessary, in order to completely understand the surface reactions, especially when we go on and try to apply the concepts obtained for material fabrications and other practical purposes.

The total flux of the incident NO is divided into the fluxes of the scattered and reacted NO. Furthermore, the flux of the reacted NO is divided into the fluxes of the gas-phase products and surface products. Therefore, we expect that the molecular-orientation dependence found in the scattered NO need not be reversed in the surface products. Thus, we perform the direct observation of the surface products created by the oriented NO beam.

In this Letter, we present direct evidence of steric effects in the dissociative adsorption of NO on Si(111), the first step in silicon-oxinitride-film formation, by monitoring the reaction-induced products on the surface with x-ray photoemission spectroscopy (XPS). The yield of the dissociated N and O atoms is larger for the N-end collision at $T_s = 330$ and 400 K than for the O-end collision, whereas the orientation effect becomes much smaller at $T_s = 600$ K. The observed steric effects also depend on the surface coverage of O and N atoms. On the basis of these

data, we suggest that the observed steric effects can be attributed to the stereodynamics in the transient trapping into a weakly bound precursor state.

The experiments were performed with an oriented-molecular-beam apparatus newly designed for XPS measurements and adapted for the orientation of NO [16]. A clean Si(111)-(7 × 7) surface (*n*-type, 1 Ω cm) was prepared by Ar⁺ sputtering and annealing at 1200 K. The pulsed NO beam (the nozzle operation: 10 Hz, 0.2 ms FWHM) was state selected in the rotational state of $|J, \Omega, M\rangle = |0.5, 0.5, 0.5\rangle$ by means of an electrostatic hexapole field [17]. The NO translational energy (E_i) can be varied from 28–240 meV for NO seeded in Kr, Ar, He, and their mixtures. The orientation of NO was constructed by a homogeneous orientation electric field (~ 10 kV cm⁻¹ [17]) in front of the surface. The total dose of NO was controlled with a shutter inserted in the molecular-beam axis. After dosing the molecular beams (without a beam stop) in the surface normal, we measured the XPS spectra of N-1s (397.1 eV) and O-1s (531.6 eV). The fractional coverage of dissociated O atoms (θ_O) was estimated from the integrated area of O-1s spectra and calibrated with the

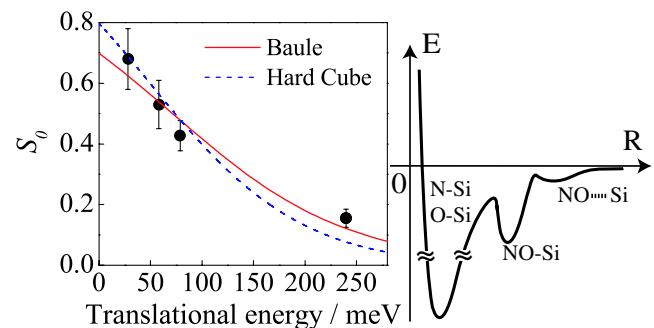


FIG. 1 (color online). (Left figure) Initial reactive sticking probability S_0 as a function of E_i for the randomly oriented NO incidence at $T_s = 400$ K. The full and dashed line represents the Baule-type and the HC models, respectively. (Right figure) Schematic interaction potential.

saturation θ_O of ~ 0.6 ML at 400 K [18]. The coverage of dissociated N atoms (θ_N) was estimated from the relative peak intensity of N-1s to that of O-1s taking the ratio of x-ray transition probability, N-1s/O-1s = 0.6 [19], and the analyzer transmission function into consideration.

Figure 1 shows the reactive sticking probability (S) obtained from the XPS-determined uptake curves of $\theta_{\text{total}}(t) = \theta_O(t) + \theta_N(t)$ for the random-orientation beams with $E_i = 28, 58, 78,$ and 240 meV at $T_s = 400$ K. Here, $S(t=0) = S_0 = \lim_{t \rightarrow 0} \frac{\theta_N(t) + \theta_O(t)}{2Ft}$ is approximated with the initial slope of the uptake curve [$\theta_{\text{total}}(t) \leq 0.2$ ML], where F and t is the flux of the beam and the exposure time, respectively. θ_N/θ_O is ~ 1 at $T_s = 400$ K independent of E_i . S_0 decreases with increasing E_i . This S_0 vs E_i can be reproduced by the Baule-type model [20] with the critical energy $E_c = 72$ meV and the hard-cube (HC) model [21] in Fig. 1. In the HC model, a NO interacts with ~ 10 Si for a 130 meV physisorption well [22]. As a result, the precursor-mediated reaction via molecular physisorption and/or chemisorption well (see Fig. 1) should be considered in this low energy region. We set the kinetic energy of NO beam to 58 meV because of the reasonably high beam stability and sticking probability. At 58 meV, good focusing condition can be attained at the hexapole voltage of ± 4.6 kV [16]. The Legendre moment $\bar{P}_n \equiv \langle P_n(\cos\gamma) \rangle$ of the orientation distribution function for the $|0.5, 0.5, 0.5\rangle$ state at 58 meV is as follows, taking the state purity into consideration: $\bar{P}_0 = 1$, $\bar{P}_1 = 0.303$, and $\bar{P}_2 = 0$, and the other higher-order terms are negligibly small. Here, γ is the angle between the orientation field and the axis of NO

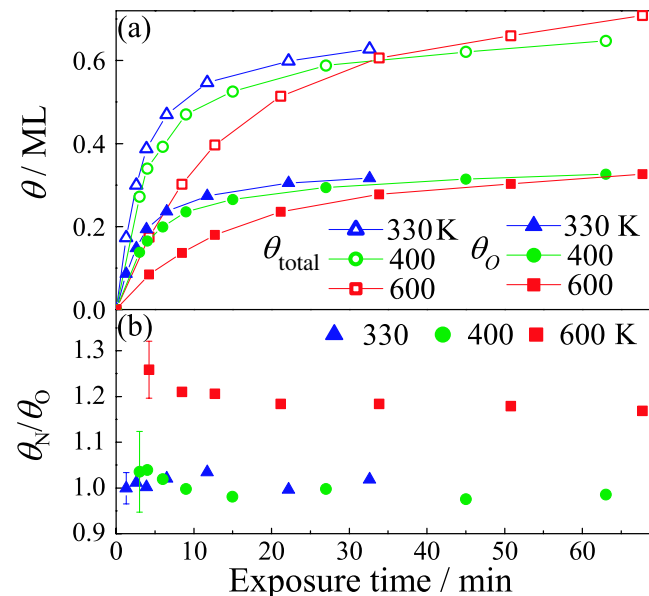


FIG. 2 (color online). (a) Uptake curves of $\theta_{\text{total}} = \theta_O + \theta_N$ and θ_O as a function of exposure time (t) for the incidence of 58 meV randomly oriented NO at $T_s = 330$ (triangles), 400 (circles), and 600 K (squares). (b) θ_N/θ_O ratio, estimated from (a), as a function of t .

defined to point from O towards N, opposite to the permanent dipole moment [23]. \bar{P}_1 corresponds to the average orientation.

Figure 2(a) shows the evolution of θ_{total} and θ_O as a function of exposure time (t) for the incidence of the 58 meV random-orientation NO $|0.5, 0.5, 0.5\rangle$ beam at $T_s = 330, 400,$ and 600 K. The T_s dependence of the uptake curve, i.e., the T_s dependence of S , also suggests that the precursor-mediated mechanism is dominant at 58 meV. No desorption of dissociatively adsorbed N and O atoms occurs at $T_s \leq 600$ K [18,24]. It is interesting that θ_N/θ_O is ~ 1 at 330 and 400 K and it increase to ~ 1.2 at 600 K, as shown in Fig. 2(b). Similar T_s dependence of θ_N/θ_O was observed in the NO exposure by backfilling [25–27]. At $T_s = 600$ K, the steric effect becomes much smaller, while θ_N/θ_O increases (*vide infra*, Figs. 3 and 4). Moreover, θ_N/θ_O does not depend on the molecular orientation. Thus, the initial molecular orientation of an incoming NO does not contribute to increase of θ_N/θ_O . The

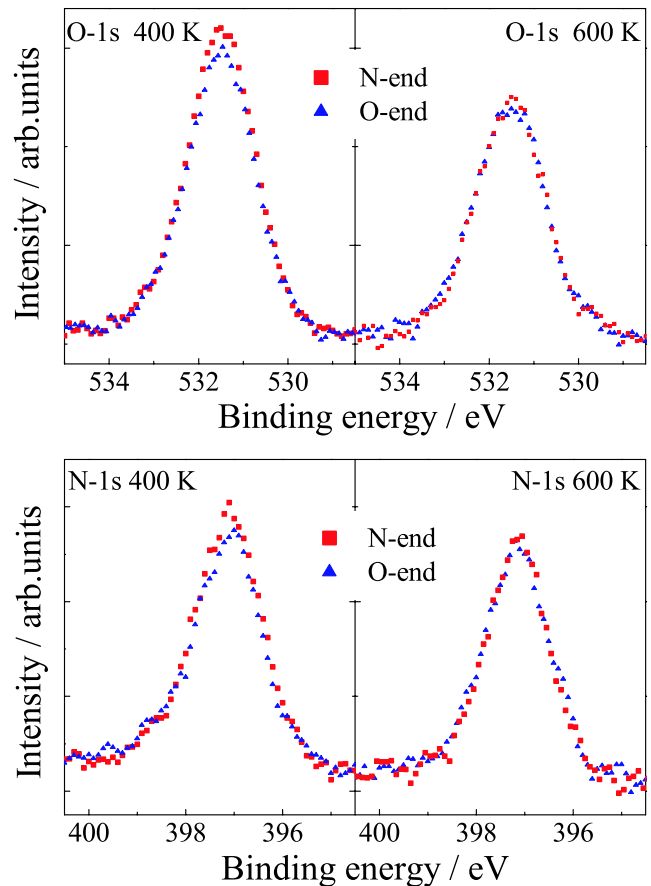


FIG. 3 (color online). Orientation dependence of the O-1s (upper) and N-1s (lower) XPS spectra for the 6 (left) and 8.5 (right) min exposures of 58 meV oriented NO beams at $T_s = 400$ (left) and 600 (right) K. The N-end and O-end collisions are indicated by squares and triangles, respectively. Spectra correspond to $\theta_{\text{total}} = \sim 0.41$ and ~ 0.30 ML at $T_s = 400$ and 600 K, respectively.

anisotropy may come from the direct reactions between stabilized NO precursors formed on the adatom and the nearest rest atom [26,27]. This is just our speculation, and will be confirmed in future studies.

Figure 3 shows the orientation dependence of the O-1s and N-1s XPS spectra, measured after the 6 (left, $\theta_{\text{total}} = \sim 0.41$ ML) and 8.5 (right, $\theta_{\text{total}} = \sim 0.30$ ML) min exposures of the 58-meV oriented NO(0.5, 0.5, 0.5) beam at $T_s = 400$ and 600 K, respectively. The beam flux was kept constant at $1.20 \times 10^{12} \text{ cm}^{-2} \cdot \text{s}^{-1}$ ($1.54 \times 10^{-3} \text{ ML s}^{-1}$) within $\pm 0.5\%$ during all measurements of steric effects. The stability of the beam flux was checked by measuring/determining the beam profile before and after each beam exposure. It is clear that an N-end collision is more reactive than an O-end collision.

Figure 4(a) shows the total coverage θ_{total} dependence of the stereo-asymmetry R . Here, we define R as follows: $R = \frac{I_N - I_O}{0.5(I_N + I_O)}$, where $I_{N,O}$ corresponds to the integrated intensity of O-1s XPS intensity at the same exposure of the N-end and O-end beams, respectively. Thus, $I_i(t_0) = F \int_0^{t_0} S_i(t) dt$, where $S_i(t)$, $i = N$ or O , is the reactive sticking probability for the N- or O-end collision, respectively. In Fig. 4(a), we plot R as a function of θ_{total} obtained at the same exposure of the random-orientation NO. We can easily observe the following: (1) R is positive and thus, it is more reactive for the N-end than the O-end collisions. (2) R depends on T_s . R becomes smaller at $T_s = 600$ K (see also Fig. 3), while θ_N/θ_O , revealing no steric effects,

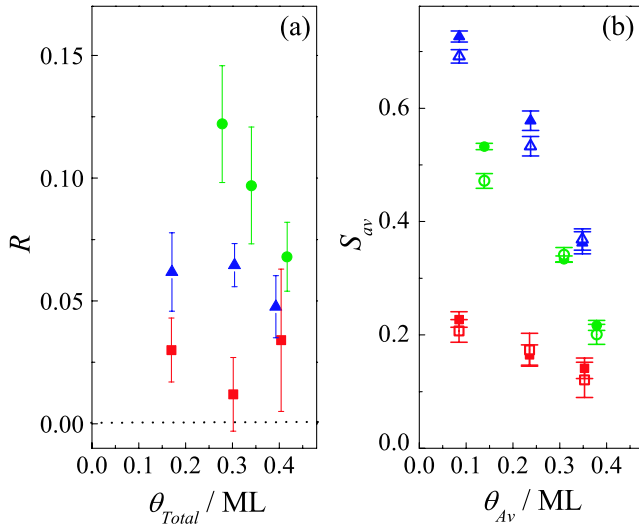


FIG. 4 (color online). (a) Stereo-asymmetry R as a function of θ_{total} at $T_s = 330$ (triangles), 400 (circles), and 600 K (squares). θ_{total} for the exposure of the random-orientation NO is used for the plot of R . (b) Average reactive sticking probability $S_{\text{av},i}$ as a function of the averaged coverage at $T_s = 330$ (triangles), 400 (circles), and 600 K (squares). $S_{\text{av},i}$ is plotted at $\theta_{\text{Av}} = \frac{\theta_{\text{total}}(t_1) + \theta_{\text{total}}(t_2)}{2}$ obtained for the dose of random-orientation NO beam. The N-end or O-end collisions are indicated as full and open marks, respectively.

becomes larger at $T_s = 600$ K. (3) R at $T_s = 400$ K is larger than at the other T_s compared at lower θ_{total} . The results (1)–(3) are also supported by the N-1s measurements.

Figure 4(b) shows the orientation dependence of reactive sticking probability $S_{\text{av},i}$ averaged with respect to θ_{total} , where $i = N$ or O denotes the N- or O-end incidence, respectively. $S_{\text{av},i}$ is defined as $S_{\text{av},i} = \frac{\theta_{\text{total},i}(t_2) - \theta_{\text{total},i}(t_1)}{2F(t_2 - t_1)}$, $t_2 > t_1$. We plot $S_{\text{av},i}$ at $\theta_{\text{Av}} = \frac{\theta_{\text{total}}(t_1) + \theta_{\text{total}}(t_2)}{2}$ for the dose of random-orientation NO beam. Molecular-orientation effects appear for $\theta_{\text{total}} < 0.25$ ML at $T_s = 330$ and 400 K. This is the origin of the positive R in Fig. 4(a). For $\theta_{\text{total}} \geq 0.25$ ML, molecular-orientation effect in S_{av} becomes smaller.

The strong T_s dependence of the uptake curves in Fig. 2(a) suggests that the precursor-mediated reaction is a dominant process in NO dissociative adsorption on Si(111). The smaller R at 600 K suggests little contribution of the direct dissociative adsorption to the steric effect. In the precursor-mediated reaction [28], two kinds of precursor potentials to the dissociative adsorption can be considered. One is a physisorption well with typical depth of ~ 130 meV [22], and the other, a molecular chemisorption well. The “atop” state (Si-N bonding), with a binding energy of 0.6–0.8 eV (estimated residence time 10^{-9} s at 400 K), is the most possible molecularly chemisorbed state into the dissociation [29]. If only trapping into the physisorption well contributes to the observed steric effect, we would expect a negative R due to the rotational excitation of NO [4]. In the case of the present study, the positive R suggests additional contribution coming from the chemisorption well. On the other hand, a strong attractive potential of chemisorption well with 0.6–0.8 eV, compared to the translational energy of 58 meV, would adiabatically reorient the NO molecule to a favorable configuration during its approach to the surface [30]. It is expected this will smear out the orientation effects. However, it should be noted that Lahaye *et al.* used a more realistic potential and demonstrated that strong reorientation does not always occur due to the orientation-dependent competition between the repulsive collision and the rotational torque, leading to some steric effects even for deep potential wells [31]. The nonadiabatic charge transfer from Si to NO [32] may also smear out orientation effects.

We believe that the moderate orientation-dependent depth of the molecularly chemisorption potential contributes mainly to the steric effect. The effective chemisorption well depth depends on where and how NO approaches at the first encounter. As the distance from the reactive site increases and the approaching geometry strays out of the stable tilted geometry [33], the potential well depth may be shallow enough as to reduce the reorientation effect on the first bounce. However, the steric dependence of the interaction potential still remains. The interaction is more attractive for the N-end approach [33]. Thus, we expect that

larger energy dissipation for the N-end approach, via transient excitations of phonons and/or electron-hole pairs in the shallow well [5,7]. Therefore, the trapping probability of NO is larger for the N-end collision and reveals the T_s dependence as a result of desorption, via excitation of surface phonons, before being trapped into further deeper chemisorption well. This orientation dependence causes the observed steric asymmetry of S at $T_s = 330$ and 400 K.

Elevating T_s to 600 K enhances the probability of desorption from transient weakly bound states via phonons, while the dissociative adsorption via the strong attractive interaction remains, the direct or strongly bound-state mediated dissociations. Both smear out the steric effects at the low energy due to the steering effect [30]. Thus, the orientation effects become smaller at high $T_s = 600$ K (see also Fig. 3). Steric effects depending strongly on T_s and E_i appeared on the trapping into the transient precursor state in $\text{CH}_3\text{Cl}/\text{Si}(100)$ [15]. The largest R at $T_s = 400$ K in Fig. 4(b), despite monotonic decrease of S with increasing T_s , suggests a similar strong dependence of steric effect on T_s .

As shown in Fig. 4(b), the steric effect decreases with increasing θ_{total} . Thus, the observed steric effect appears via an intrinsic precursor well, i.e., direct interaction with the substrate. The repulsive interaction of incident NO with the preadsorbed N and O atoms reduces the interaction length and the strength of attractive interaction in the precursor well. As a result, the anisotropy of NO becomes smaller at high coverage.

In summary, we found the steric effects in NO/Si(111) by monitoring the oriented-beam induced products *on the surface* with XPS. The orientation-dependent trapping of NO into the shallow precursor well can explain the observed steric effect. The technique combining the oriented molecular beam and XPS will be a powerful tool for the study of the stereodynamics in the various chemical reactions on complex systems.

We gratefully acknowledge MEXT for a Nanotechnology Research Project and for a Grant-in-Aid for Scientific Research (No. 20350005). M.O. was also financially supported by PRESTO of JST.

*Corresponding author.

okada@chem.sci.osaka-u.ac.jp

- [1] E. W. Kuipers *et al.*, Nature (London) **334**, 420 (1988).
- [2] E. W. Kuipers *et al.*, Phys. Rev. Lett. **62**, 2152 (1989).
- [3] G. H. Fecher *et al.*, Surf. Sci. Lett. **230**, L169 (1990).
- [4] M. G. Tenner *et al.*, Surf. Sci. **242**, 376 (1991).
- [5] H. Müller *et al.*, Chem. Phys. Lett. **223**, 197 (1994).
- [6] H. Müller *et al.*, Surf. Sci. **307–309**, 159 (1994).
- [7] M. Brandt *et al.*, Surf. Sci. **331–333**, 30 (1995).
- [8] H. Hou *et al.*, Science **277**, 80 (1997).
- [9] R. S. Mackay *et al.*, J. Chem. Phys. **92**, 801 (1990).
- [10] M. Brandt *et al.*, Phys. Rev. Lett. **81**, 2376 (1998).
- [11] W. A. Diño *et al.*, Phys. Rev. Lett. **78**, 286 (1997).
- [12] A. J. Komrowski *et al.*, J. Chem. Phys. **117**, 8185 (2002).
- [13] L. Vattuone *et al.*, Angew. Chem., Int. Ed. **43**, 5200 (2004).
- [14] A. Gerbi *et al.*, Angew. Chem., Int. Ed. **45**, 6655 (2006).
- [15] M. Okada *et al.*, Phys. Rev. Lett. **95**, 176103 (2005); J. Am. Chem. Soc. **129**, 10052 (2007).
- [16] See EPAPS Document No. E-PRLTAO-101-006827 for experimental details. For more information on EPAPS, see <http://www.aip.org/pubservs/epaps.html>.
- [17] M. G. Tenner *et al.*, Surf. Sci. **236**, 151 (1990).
- [18] P. Gupta *et al.*, Phys. Rev. B **40**, 7739 (1989).
- [19] C. D. Wagner *et al.*, *Handbook of X-Ray Photoelectron Spectroscopy* (Perkin Elmer/Physical Electronics Division, Eden Prairie, MN, 1979).
- [20] C. T. Rettner *et al.*, J. Chem. Phys. **90**, 3800 (1989).
- [21] E. W. Kuipers *et al.*, Surf. Sci. **205**, 241 (1988).
- [22] C. E. Brown and P. G. Hall, J. Colloid Interface Sci. **42**, 334 (1973).
- [23] A. Gijsbertsen *et al.*, Phys. Rev. Lett. **99**, 213003 (2007).
- [24] A. G. Schrott and S. C. Fain, Jr., Surf. Sci. **111**, 39 (1981).
- [25] M. Nishijima *et al.*, Surf. Sci. **137**, 473 (1984).
- [26] M. Hashinokuchi *et al.*, Jpn. J. Appl. Phys. **47**, 1672 (2008).
- [27] M. D. Wiggins *et al.*, J. Vac. Sci. Technol. **18**, 965 (1981).
- [28] W. H. Weinberg, in *Kinetics of Interface Reactions*, edited by M. Grunze and H. J. Kreuzer (Springer, New York, 1987), p. 94.
- [29] Z. C. Ying and W. Ho, J. Chem. Phys. **91**, 2689 (1989).
- [30] C. W. Muhlihausen *et al.*, J. Chem. Phys. **83**, 2594 (1985).
- [31] R. J. W. E. Lahaye *et al.*, J. Chem. Phys. **104**, 8301 (1996).
- [32] M. A. Rezaei *et al.*, J. Chem. Phys. **110**, 4891 (1999).
- [33] Z. Su *et al.*, Chem. Phys. Lett. **375**, 106 (2003).